U.S. CLIVAR VARIATIONS

Fall 2005, Vol. 3, No. 3

Focus on Extremes

by David M. Legler, Director

Fall is upon us, and with it comes the start of schools and universities, and after the traditional vacation period, a refreshed (I hope!) research community. Fall is also the time when the new Fiscal Year begins and agencies begin allocating and planning to spend their FY2006 appropriations (when Congress and the President can agree on them), proposing (internally) budgets for FY2007, and planning for FY2008 and beyond. The next six months are a critical time for U.S. CLIVAR to provide input to the federal research agencies.

In past issues of Variations, I have highlighted the motivation for reorganizing the structure of U.S. CLIVAR and how such changes would be carried out. At our first annual meeting (or Summit), the new organizational units met to take U.S. CLIVAR forward (a report on the Summit appears elsewhere in this issue). The meeting was a very positive one from several points of view and I anticipate the invigorating scientific discussion, increased energy, and engagement by both the scientists and agency

Continued on Page Two

IN THIS ISSUE

On the Relationship Between ENSO and Extreme Weather Over the Contiguous U.S.

Siegfried D. Schubert, Yehui Chang[1], Max Suarez and Philip Pegion[2]
NASA/GSFC, Earth-Sun Exploration Division, Greenbelt, Maryland
[1] Goddard Earth Sciences and Technology Center, University of Maryland Baltimore County, Baltimore, Maryland
[2] Science Applications International Corporation, Beltsville, Maryland

1. Introduction

Global-scale climate variations such as those associated with El Niño/Southern Oscillation (ENSO) are ultimately manifest in phenomena and processes that control regional-scale climates. For example, shifts in the wintertime planetary scale waves forced by tropical sea surface temperature (SST) anomalies can result in changes in the normal tracks and frequencies of storm systems (e.g. Noel and Changnon 1998) which can result in dramatic changes in regional climates of North America. Any potential changes in extreme weather events are of particular concern since these tend to have the greatest economic and social consequences. It is therefore of interest to determine whether the characteristics of extreme events are influenced by short-term climate variability such as that associated with ENSO. For example, Gershunov and Barnett (1998) and Gershunov (1998) show that the frequency of heavy rainfall is impacted by ENSO in a number of regions of the United States including the Great Plains, the Southeast, and the Gulf States. Cayan et al. (1999) show that ENSO impacts the occurrence of extreme (heavy) daily precipitation and stream flow throughout the western United States.

One limitation of many recent studies of weather extremes is that the analysis of the extreme events is carried out local in space, with little information provided about the underlying phenomenology and mechanisms associated with the extremes. In the case of precipitation, Web and Betancourt (1992) emphasize that understanding the hydroclimatic controls on flood frequency requires understanding the modulation of the flood generating mechanisms: for example, frontal systems, monsoonal flows and tropical storms. In that sense, identifying the impact on weather is an important step in determining the physical mechanisms by which short term climate variations impact extremes.

In this study, we examine the impact of ENSO on extreme precipitation events associated with winter storms over the continental United States. By extreme value we mean here the maximum daily value over the course of a winter season. The results are based on observations (Higgins et al 1996), and an ensemble of nine atmospheric general circulation model (AGCM) simulations forced with observed SST for the 50-year period 1949-98. The AGCM is the NASA Seasonal to Interannual Prediction Project (NSIPP-1) model described in Bacmeister et al. (2000) and run here at a resolution of 2° latitude by 2.5° longitude. The nine runs differ only in their initial atmospheric con-

Continued on Page Two

Continued from Page One

representatives is the start of an era of increased effectiveness for the program.

I am saddened to report that Mike Patterson, program manager in NOAA's Office of Global Programs, will be taking an extended leave of absence from NOAA for the foreseeable future. Mike has been a critical supporter of U.S. CLIVAR and VAMOS efforts. It has been my pleasure to have worked with Mike for the past several years. I now look forward to working with Jin Huang, program manager for the NOAA CPPA program. I hope you will join me in welcoming her to the U.S. CLIVAR program.

In recent days the destructive power of hurricanes has been documented in the mass media; their impact brought closer to us through first-hand stories of survival and resilience. A hurricane is one type of an "extreme" event (other extreme events include prolonged anomalous temperatures, droughts, and floods) that is by its nature infrequent, but often very calamitous. In this issue we present a few reports on the connection between extreme weather and ENSO, of the likelihood of extremes in coupled climate model runs, and shifts in multidecadal patterns leading to potential changes of regionally important extreme events.

Variations

Published three times per year
U.S. CLIVAR Office
1717 Pennsylvania Ave., NW, Suite 250
Suite 250, Washington, DC 20006
(202) 419-3471
usco@usclivar.org

Staff: ; , ?4 0260; , *Editor*
, =3B) =0: 308<,
Assistant Editor and Staff Writer

This newsletter is supported through contributions to the U.S. CLIVAR Office by NASA, NOAA—Office of Global Programs, and NSF.

ENSO and Extreme Weather Over the Contiguous U.S.

Continued from Page One

ditions: these were chosen arbitrarily from previously completed simulations.

An empirical orthogonal function (EOF) analysis of daily precipitation data is carried out separately for the observations and simulations to isolate the leading modes of precipitation variability. For both the observations and simulations, the first six rotated EOFs consist of localized precipitation anomalies that emphasize variability along the west coast, and the southern and southeast United States, and account for more than 50% of the variance over much of these regions. In the case of the observations, we find that the leading EOFs can be identified with many of the major winter storms that have occurred over the continental United States during the last 50 years. We focus here on those storms that contribute to extreme precipitation events along the gulf coast (the GC EOF) and the east coast (the EC EOF). These storms are well simulated, and the ensemble of runs provides a large sample of extreme events for statistical analysis. In the observations, the GC and EC storms show up as EOFs 3 and 4, respectively. In the EOF analysis of the model simulations, the GC and EC storms show up as EOFs 6 and 4, respectively. The model EOFs do have substantially less variance compared with the observed (the ratio of simulated to observed variance is 0.34 for the GC EOF and 0.45 for the EC EOF). This is likely a result of the relatively coarse resolution of the model.

2. The impact of ENSO

In this section we examine the impact of ENSO on the extreme values of the PCs associated with the GC and EC EOFs. We begin by ordering the years according to the overall level of activity of the storms during each winter (measured by the variance of the PCs – see Table 1). Both the observations and simulations show a predilection for enhanced activity in the GC and EC storms during El Niño winters, while suppressed activity in the GC storm tends to occur during La Niña years. The simulated EC storms also tend to be suppressed during La Niña years, while that is less true for the observations.

We next examine how ENSO impacts the winter maxima by fitting the daily maxima to a class of extreme value distributions. In particular, we fit the maximum values *(x)* to the Generalized Extreme Value (GEV) cumulative distribution function (Coles 2001)

$$G(x) = \exp\left\{-\left[1+\zeta\left(\frac{(x-\mu)}{\sigma}\right)\right]^{-1/\zeta}\right\},$$

with location parameter (μ), scale parameter (□), and shape parameter □. Here

$$\{x : 1+\zeta(x-\mu)/\sigma > 0\}, \quad -\infty < \mu,\zeta < \infty$$

and □ >0. The Gumbel distribution (□=0) is one of three submodels of the GEV, the other two being the Fre`chet (□=0) and reverse Weibull (□ >0). The N-year return value for the GEV distribution (the value that is on average exceeded once in N-years) is,

$$X_N = \mu - \frac{\sigma}{\zeta}\left\{1-\left[-\ln\left(1-\frac{1}{N}\right)\right]^{-\zeta}\right\}$$

We found that, for the observations, the Gumbel distribution provides a reasonable representation of the distribution of the maximum values of the PCs. On the other hand, we found that the reverse Weibull distribution provided the best fit to the leading simulated PCs. It is not clear whether this represents a real difference between the model and observations or whether the limited sample size (49 winters) of the observations is simply insufficient to produce a statistically significant estimate of the shape parameter.

In order to examine the impact of ENSO, we carry out the extreme value analysis separately for the La Niña, neutral and El Niño years. The impact of ENSO is quantified by computing an effective return period N* (Katz et al. 2002), defined for the GEV distribution as

$$N^* \equiv \left\{1-\exp\left(-\left[1+\zeta^*\frac{X_N-\mu^*}{\sigma^*}\right]^{-\frac{1}{\zeta}}\right)\right\}^{-1}$$

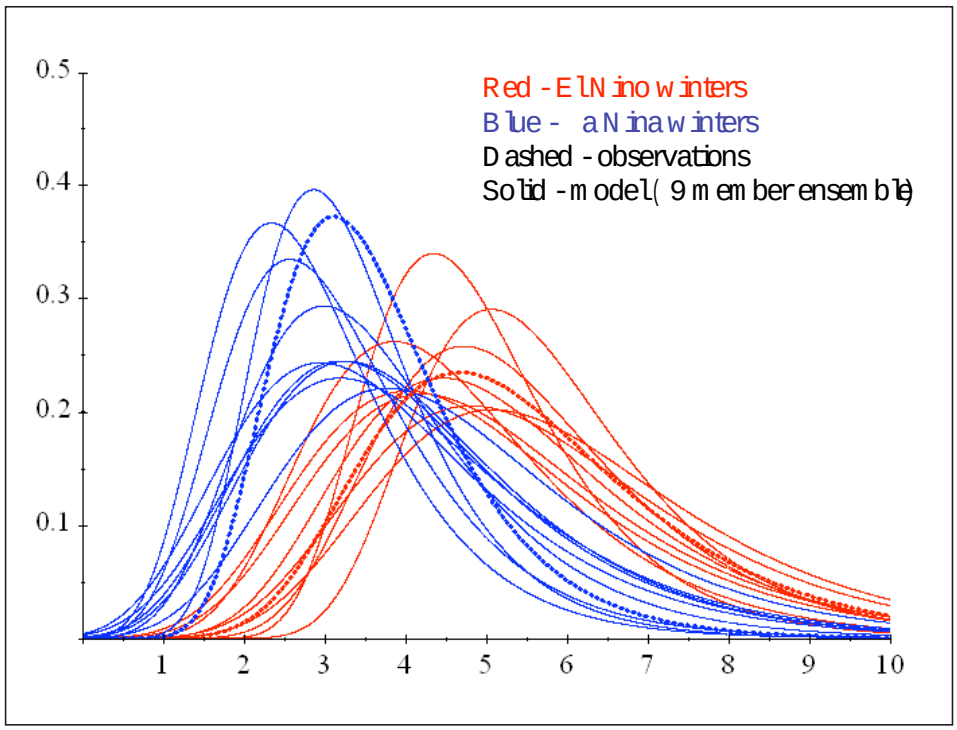

Figure 1: Probability Density Functions (PDFs) of extreme winter storms that tend to develop along the Gulf Coast (GC) during DJF (1949-1998). The PDFs correspond to the maximum value of the principal components associated with EOF 3 (observations) and EOF 6 (model). Values are scaled so that the model and observed EOFs have the same total variance. Units are arbitrary. The PDFs are the fits to a Gumbel Distribution. The analysis was done using the XTREMES software package (Reiss and Thomas 1997).

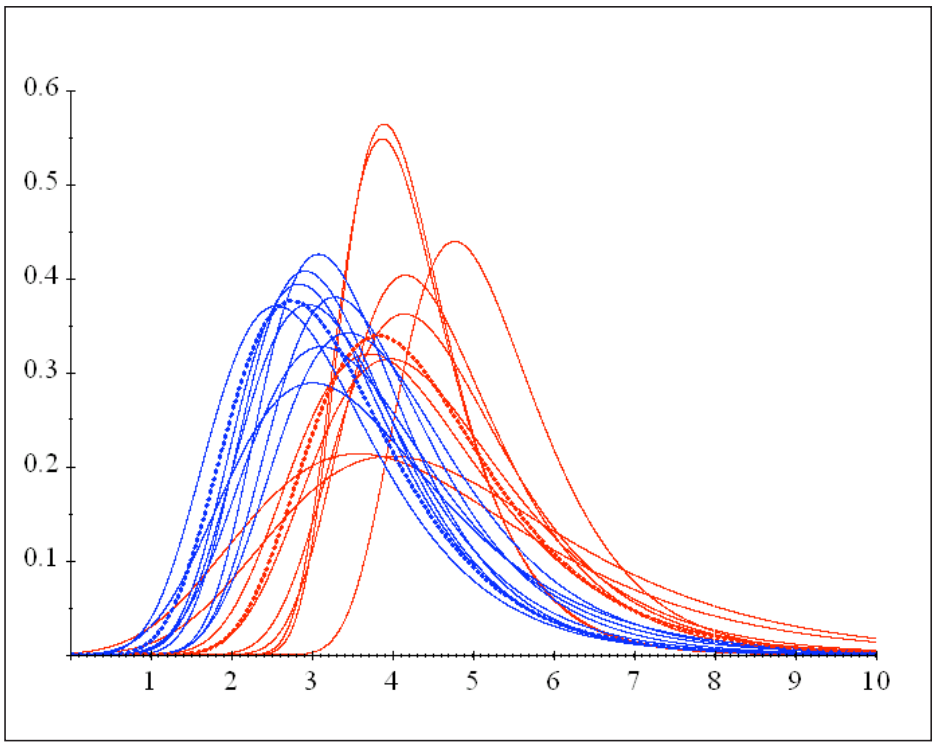

Figure 2: Same as Fig.1, except for the extreme winter storms that develop along the east coast (EC). The PDFs correspond to the maximum value of the principal components associated with EOF 4 (observations) and EOF 4 (model).

where the star (*) indicates conditional parameter values, and X_N is the unconditional N-year return value For example, one might compute X_N from a full record, and then recalculate the parameters only for El Niño years. In that way one can more readily quantify the impact of El Niño in terms of the change in the return period.

The results for the GC and EC principal components are shown in Table 2. For the observations, only the location parameter, μ, is impacted by ENSO – there are no significant impacts from ENSO on the scale parameter, σ. In fact, we take advantage of this result by fixing the scale parameter to be that estimated from the full (unconditional) record, thereby reducing the number of free parameters in the final fit. Both the GC and EC storms have significantly different location parameters during cold and warm years. The impact is quantified in the last column in Table 3 in terms of the impact on the return values. The results are such that observed extreme GC and EC storms that occur on average only once every 20 years (20-year storms) would occur on average in half that time under El Niño conditions. In contrast, under La Niña conditions, 20-year GC and EC storms would occur on average about once in 30 years. The results are quite similar for the *simulated* GC storms in that the 20-year return values would occur on average in half that time during warm years, and twice that time during cold years. For the EC storms the 20-year return value would also occur in half that time under warm conditions and in about twice that time under cold conditions.

Figure 1 shows the results of fitting Gumbel distributions to the observations and each of the 9 ensemble members. We choose here to fit the simpler Gumbel distribution to the model results since, by doing the fits to the individual ensemble members, we are limiting the sample size to that of the observations. The scatter among the ensemble members gives an indication of the sampling errors. The fact that the fit to the observations falls within the scatter suggests that the model results are quite realistic. The results also show that the impact from ENSO clearly separates the warm and cold years (despite the sampling errors), with La Niña years tending to produce considerably less

88-89	**88-89**	**88-89**	*49-50*
70-71	75-76	*49-50*	59-60
93-94	70-71	*79-80*	*50-51*
74-75	**73-74**	85-86	**88-89**
75-76	*49-50*	*87-88*	75-76
59-60	59-60	*50-51*	*95-96*
61-62	53-54	56-57	**73-74**
50-51	60-61	*55-56*	60-61
49-50	*50-51*	68-69	52-53
67-68	96-97	80-81	70-71
62-63	*84-85*	51-52	*55-56*
56-57	*64-65*	*64-65*	80-81
85-86	*74-75*	*95-96*	85-86
73-74	*95-96*	61-62	71-72
84-85	*55-56*	70-71	89-90
94-95	78-79	*75-76*	*64-65*
69-70	80-81	52-53	51-52
68-69	*79-80*	62-63	61-62
55-56	56-57	76-77	78-79
83-84	71-72	96-97	*84-85*
52-53	66-67	53-54	*79-80*
89-90	62-63	93-94	*74-75*
95-96	*83-84*	60-61	81-82
60-61	67-68	67-68	*90-91*
96-97	63-64	71-72	53-54
66-67	85-86	*69-70*	96-97
79-80	*54-55*	*84-85*	62-63
72-73	89-90	*74-75*	56-57
71-72	81-82	**91-92**	66-67
80-81	**57-58**	*58-59*	63-64
51-52	51-52	*54-55*	*83-84*
57-58	68-69	*83-84*	68-69
81-82	*69-70*	89-90	*92-93*
63-64	*87-88*	72-73	*54-55*
87-88	52-53	*77-78*	67-68
53-54	*90-91*	*90-91*	*65-66*
64-65	65-66	66-67	*77-78*
58-59	*77-78*	**73-74**	*69-70*
76-77	61-62	**57-58**	*58-59*
92-93	*58-59*	65-66	**57-58**
86-87	76-77	81-82	*87-88*
54-55	93-94	94-95	76-77
65-66	**91-92**	*92-93*	**91-92**
77-78	**97-98**	63-64	94-95
78-79	*92-93*	86-87	72-73
91-92	72-73	59-60	86-87
90-91	94-95	78-79	93-94
82-83	86-87	**82-83**	**97-98**
97-98	**82-83**	**97-98**	**82-83**

Table 1: List of the winters (DJF) ordered by increasing variance for the GC and EC PCs from the observations and model simulations. Blue indicates La Niña years, and red indicates El Niño years. Bold indicates major events. Italics indicate weak events. The classification of the years into warm and cold events is that of the Climate Prediction Center (the classification scheme is subjective and is based on SST analyses; http://www.nnic.noaa.gov)

intense extremes than the El Niño years.

Fig. 2 is the same as Fig. 1, except for the EC storms. Here again we see that the fits to the observed values fall within the scatter of the fits to the individual ensemble members. The cold and warm years are also clearly separated, though in this case there is considerably more scatter in the results for the warm years, with some ensemble members showing a quite broad distribution, while others are more narrow and peaked.

PC	ENSO	μ – location	σ – scale	ζ – shape	N*
	cold	3.71 (3.1, 4.6)	1.59		30.0
GC (obs)	neutral	4.30 (3.8, 4.9)	1.59		20.9
	warm	5.26 (4.7, 6.1)	1.59		11.6
	cold	3.37 (0.16)	1.57 (0.12)	-0.04 (0.08)	33
GC(sim)	neutral	4.29 (0.14)	1.76 (0.10)	-0.16 (0.05)	28
	warm	5.18 (0.18)	1.88 (0.12)	-0.15 (0.06)	10
	cold	3.49 (3.0, 4.2)	1.25		29.7
EC(obs)	neutral	4.09 (3.7, 4.6)	1.25		18.7
	warm	4.77 (4.3, 5.3)	1.25		11.0
	cold	3.81 (0.13)	1.34 (0.09)	-0.06 (0.05)	43
EC(sim)	neutral	4.13 (0.11)	1.38 (0.08)	-0.04 (0.04)	26
	warm	5.05 (0.15)	1.58 (0.09)	-0.10 (0.03)	11

Table 2: The parameter estimates of the GEV distribution for the EC and GC PCs from the observations and model simulations. Values are based on the maximum daily values during DJF based on either the 50 (1949-98) observed winters or the 450 simulated winters comprised of nine ensemble members times fifty (1949-98) years. Separate fits are done for La Niña, neutral and El Niño winters. For the observations, the values in parentheses are the 90% confidence intervals based on 2000 Monte Carlo simulations. For the simulations, the values in parentheses are the standard errors. Parameter values (μ, ¤) are normalized by the standard deviation of the PCs. The last column shows the effective return period (in years) that the X_{20} value would have under warm, cold, or neutral ENSO conditions. The results were computed using either the XTREMES software package (Reiss and Thomas 1997), or the extRemes software described at http://www.assessment.ucar.edu/toolkit/index.html.

Acknowledgements:

This work was supported by the NASA Earth Science Enterprise's Global Modeling and Analysis Program.

References

Bacmeister, J., P.J. Pegion, S. D. Schubert, and M.J. Suarez, 2000: An atlas of seasonal means simulated by the NSIPP 1 atmospheric GCM, NASA Tech. Memo. No. 104606, volume 17, Goddard Space Flight Center, Greenbelt, MD 20771, 2000.

Cayan, D. R., K.T. Redmond, and L.G. Riddle, 1999: ENSO and hydrological extremes in the western United States. *J. Climate*, , 2881-2893.

Coles, S. 2001: An Introduction to Statistical Modeling of Extreme Values. Springer Verlag, London.

Gershunov, A., 1998: ENSO influence on intraseasonal extreme rainfall and temperature frequencies in the continguous United States: Implications for long-range predictability. *J. Climate*, , 3192-3203.

Gershunov, A. and T.P. Barnett, 1998: ENSO influence on intraseasonal extreme rainfall and temperature frequencies in the continguous United States: Observations and model results. *J. Climate*, , 1575-1586.

Higgins, R. W., J. E. Janowiak and Y. Yao, 1996: A gridded hourly precipitation data base for the United States (1963-93). NCEP/Climate Prediction Center, Atlas No. 1.

Kalnay, E., and Coauthors, 1996: The NCEP/NCAR 40-year reanalysis project. *Bull. Amer.Meteor.Soc.*, , 437-471.

Katz, Richard W., Parlange, Marc B. and Naveau, Philippe, 2002: Statistics of extremes in hydrology. *Advances in Water Resources*, #, 1287–1304.

Noel, J. and D. Changnon, 1998: A pilot study examining U.S. winter cyclone frequency patterns associated with three ENSO parameters. *J. Climate*, , 2152-2159.

Reiss, R.-D., and M. Thomas, 1997: Statistical Analysis of Extreme Values. Birkhäuser, Basel, 316 pp.

Webb, R.H. and J.L. Betancourt, 1992: Climate variability and flood frequency of the Santa Cruz River, Pima County, Arizona. U.S. Geological Survey, Water-Supply Paper, 2379. 40pp.

Yarnal, B. and H.F. Diaz, 1986: Relationships between extremes of the Southern Oscillation and the winter climate of the Anglo-American Pacific coast. *J. Climate.*, , 197-219.

Changes in Daily Precipitation and Surface Air Temperature Extremes in the IPCC AR4 Models

Michael Wehner, Scientific Computing Group
Computational Research Division Lawrence Berkeley National Laboratory
1 Cyclotron Road, MS-50F Berkeley, CA 94720
(510) 495-2527; mfwehner@lbl.gov

Extreme weather events can have serious impacts on human and ecological systems. In this paper, predicted twenty-first century changes in the twenty year return value of seasonal maximum daily averaged precipitation and annual maximum daily averaged surface air temperature are calculated from the archived results of the IPCC AR4 models.

The projected likelihood of changes in extreme weather events as the mean climate changes over the course of the coming decades is high. However, the ability of the current generation of climate models to predict changes in extreme weather is largely untested. Extreme value theory provides a rigorous statistical formalism to quantify how climate models simulate extreme weather events as well as what they tell us about the predicted changes in such events. The definition of "extreme" is somewhat arbitrary as what might be considered extreme at one place and time might be quite ordinary somewhere else. Likewise, the impact of an extreme event of any given size depends greatly on the context in which it occurs. Often investigators consider events in the upper five or ten percentiles of the distribution of possible events to be extreme (for instance, Easterling, et al. 2000). However in this paper, we follow the formalism of Zwiers and Kharin (1998) and consider extreme events to be much rarer occurrences. The extreme values of a random variable, when precisely defined, are also random variables. Extreme value statistical theory (Leadbetter et al. 1983) dictates that under very general assumptions regarding the parent distribution, the values in its tail must obey well defined distribution functions. If extreme events are defined to be the maximum or minimum value encountered over a fixed period of time, for instance seasonally or annually, the Generalized Extreme Value (GEV) distribution function appropriately describes the distribution of such extreme values (Castillo, 1988). By further considering the tail of the appropriate GEV distribution, one is truly describing rare events.

The GEV distribution, F(x), is a three parameter function,

$$F(x) = \begin{cases} e^{-\left[1-k(x-\xi)/\alpha\right]^{1/k}} & k \neq 0 \\ e^{-e^{-(x-\xi)/\alpha}} & k = 0 \end{cases} \quad (1)$$

where □, □ and □ are called the location, scale and shape factors. The Gumbel distribution is a special case where the shape parameter, □, is zero. *F(x)* is the limiting cumulative distribution function of the maxima of a sample of independently and identically distributed random variables such as the annual or seasonal extrema of a sample of daily averaged fields (Leadbetter et al. 1983). The three parameters of the GEV distribution may be quickly and accurately estimated from a sample of extreme values using a technique based on L-moments (Hosking and Wallis 1997).

The return value of a random variable, X_T is that value which is exceeded, on average, once in a period of time, T. For example, when considering annual maxima of daily averaged variables, there is a 1/T chance of any daily average exceeding X_T in a given year (where T is in years). Formally, this is straightforwardly defined as

$$F(X_T) = 1 - 1/T \quad (2)$$

Solving for X_T using the above definition of the GEV distribution yields,

$$X_T = \begin{cases} \xi + \alpha[1 - \{-\ln(1-1/T)\}^k]/k & k \neq 0 \\ \xi - \alpha \ln(-\ln(1-1/T)) & k = 0 \end{cases} \quad (3)$$

Hence, return values of annual extrema are readily obtained by this inversion of the GEV distribution after its three parameters have been estimated.

In preparation for the Fourth Assessment Report (AR4) of the Intergovernmental Panel on Climate Change (IPCC), the world's leading climate modeling groups have performed a suite of integrations under common forcing conditions. Data from these simulations have been quality controlled and archived by the Program for Climate Model Diagnosis and Intercomparison (PCMDI) at the Lawrence Livermore National Laboratory. A subset of the modeling groups submitted daily output, and some of the groups even submitted data from ensembles of integrations.

Individual integrations of a single model differing only in initial conditions are statistically independent and identically distributed. The annual maxima over a given period may be straightforwardly obtained for each realization. In transiently forced numerical experiments, if the period is short enough to ignore trends in the data, these sets of extrema may be concatenated to increase the sample size and reduce the

Figure 1: a) Mean model predicted change (Kelvins) of the twenty year return value of the annual maximum daily averaged surface air temperature. The period considered is 1990-1999 to 2090-2099. b) Difference (Kelvins) between the predicted change in twenty year return values and the warmest seasonal mean values obtained for surface air temperature from the mean model ensemble. The period considered is 1990-1999 to 2090-2099. c) The number of times on average over a twenty year period that the 1990-1999 annual maximum daily averaged surface air temperature twenty year return value levels would be reached under the SRES A1B 2090-2099 forcing conditions over twenty years. Under 1990-1999 forcing conditions, this value is defined to be one.

Figure 1a

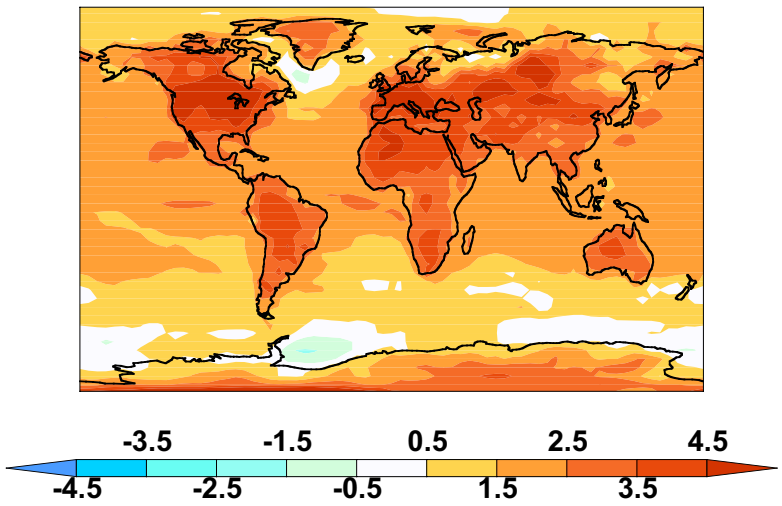

Figure 1b

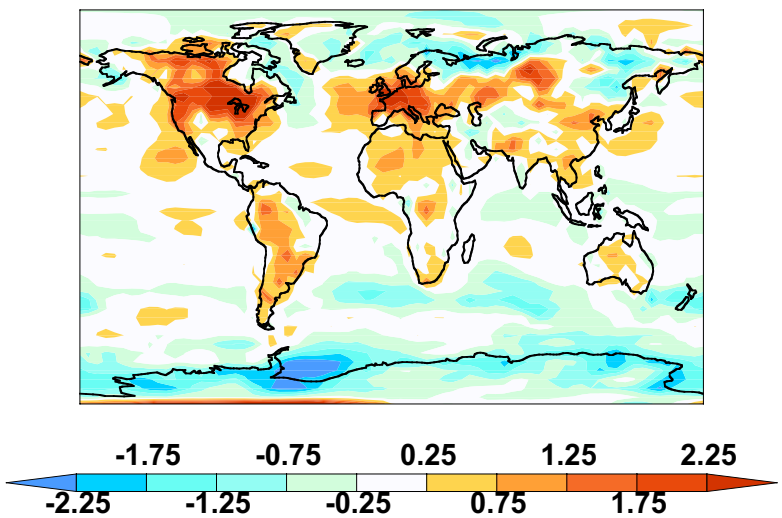

Figure 1c

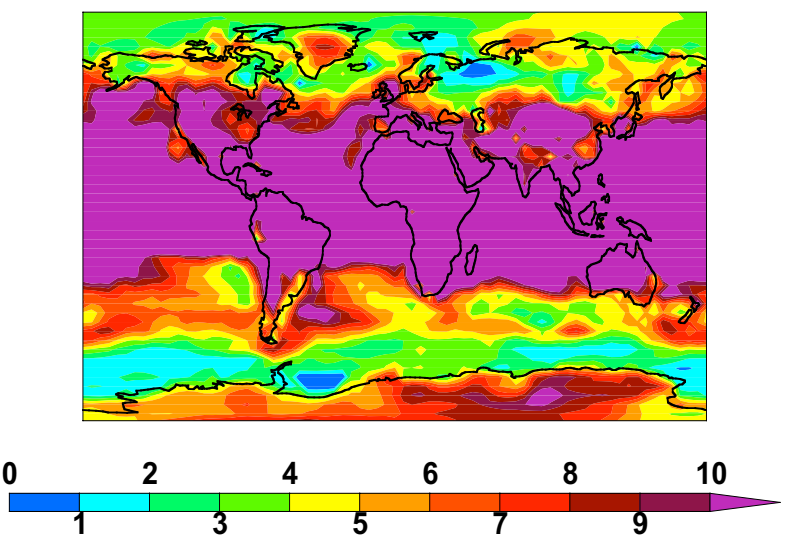

uncertainty in the estimation of GEV distribution parameters. In this study, the focus is on single decades at the ends, i.e. 1990-2000, and 2090-2099, of the "climate of the twentieth century" (20c3m) and the "SRES A1B scenario" (sresa1b) which is the 750 ppm stabilization scenario.

Output from different models may also be combined to form a multi-model ensemble. Such techniques often yield climatological results that are in better agreement with reality than any single model (Taylor, et al 2005). The procedure used in this study weighted each model equally regardless of the number of available realizations. Because each individual model has different biases, the models' annually averaged values were subtracted from the corresponding extrema and the mean model's annually averaged values added back to the result. For those models with multiple realizations, the maxima of each individual realization were calculated prior to this step and a single-model ensemble average of these maxima formed. Regridding to the coarsest model's horizontal resolution completed the construction of the multi-model ensemble. Hence, the number of multi-model "realizations" equals the number of individual models considered.

The model results in the IPCC AR4 database span a wide range of resolutions and sensitivity to atmospheric forcing changes. Those modeling groups that contributed daily averaged datasets are summarized in Table 1.

The change in the multi-model twenty year return value of daily averaged surface air temperature from the end of the twentieth century (1990-1999) to the end of the twenty-first century (2090-2099) is shown in figure 1a under the A1B SRES scenario forcing conditions. Positive changes (indicating warming) are seen almost everywhere except in two polar ocean locations. The largest changes are over land in the Northern Hemisphere. In Europe, Southern Canada and parts of the continental United States, changes in the return value exceeding five Kelvins are widespread. The overall spatial pattern of changes in the extreme values of surface air temperature mimics that of changes in the relevant mean values. For both the multi-model and single model ensemble cases, the centered pattern correlation

Figure 2a

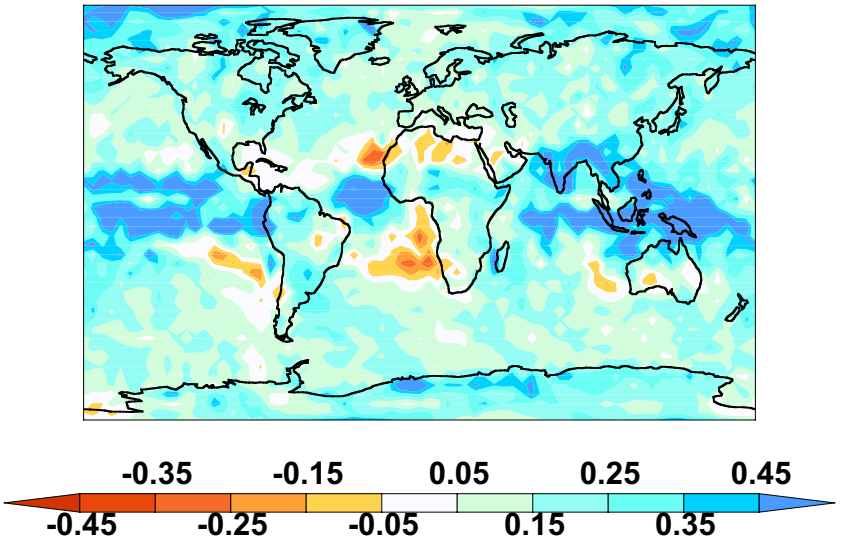

Figure 2b

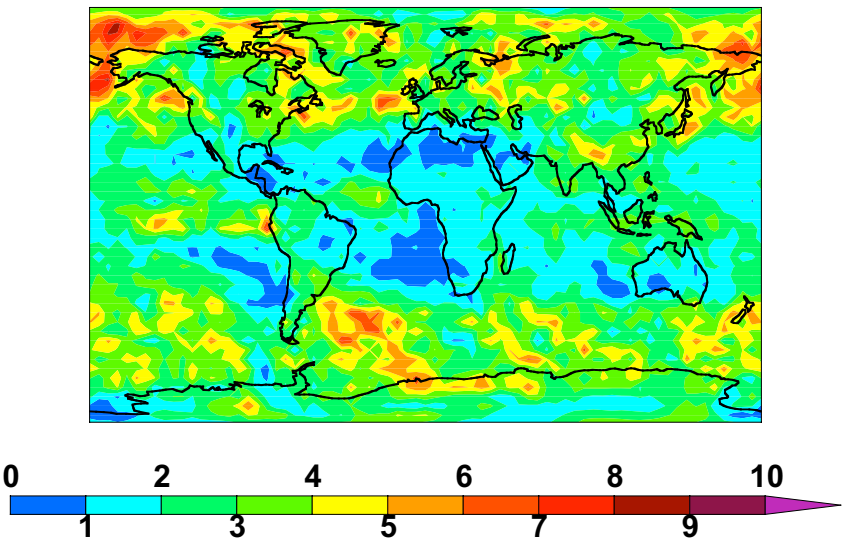

Figure 2: a) Predicted fractional change of the twenty year return value of the annual maximum averaged daily precipitation. The period considered is 1990-1999 to 2090-2099. b) The number of times on average over a twenty year period that the 1990-1999 annual maximum daily averaged precipitation twenty year return value levels would be reached under the SRES A1B 2090-2099 forcing conditions over twenty years. Under 1990-1999 forcing conditions, this value is defined to be one.

Model	Number of realizations		Atmospheric sub model Resolution
	20c3m	sresa1b	
CCSM3.0	8	4	T85L26
MRI3.2	5	5	T42L30
PCM	4	4	T42L17
MIROC3.2	3	3	T42L19
CSIRO	2	2	T63L18
CCCMA	1	1	T47L31
GISS ER	1	1	5^ox4^oL20
GISS AOM	1	1	4^ox3^oL12
GFDL CM2.0	1	1	~2.5^ox~2^oL24
GFDL CM2.1	1	1	~2.5^ox~2^oL24
Multi-model	10	10	5^ox4^o

Table 1: IPCC AR4 modeling groups that contributed daily averaged data sets.

factor between the changes in return value and the changes in the decadal average of the hot season (either JJA or DJF) factor exceeds 0.8. However, this is not to imply that the extreme value changes are identical to the mean value changes. In figure 1b, the difference between the twenty year return value changes and the changes in the hot season decadal mean are plotted revealing spatially consistent regions over land where the return values changes are up to two Kelvins higher than the mean value changes. Interestingly, the negative changes seen in the multi-model return value changes do not appear in the single model ensemble results for return value changes but rather come from large contributions from single realization models. These negative changes are also not manifested in the mean model hot seasonal mean changes suggesting that these regions may be noisy and require more integrations.

The twenty year return value represents rare events, likely to occur only a few times over the course of an individual's lifetime. The predicted large changes in surface air temperature extremes would likely have significant impacts. Another way to gauge the magnitude of these changes is to consider the change in frequency of a given size event. Upon determination of the GEV distribution, this may be straightforwardly determined by calculating the return time, T, from equation 2. The twenty year return value increases of figure 1a imply that the end of twentieth century levels would be realized on average far more often than once over that return period at the end of the twenty first century. Figure 1c show how many times on average over a twenty year period that the 1990-1999 return value levels would be reached under the SRES A1B 2090-2099 forcing conditions. Over much of the globe, present day rare events would become commonplace, often occurring on average more than ten times over the twenty years.

Changes in precipitation extremes are postulated to be related to changes in atmospheric temperature (Allen and Ingram, 2002). For as the atmosphere warms, it can potentially hold more moisture. Extreme precipitation events occur when large fractions of the total moisture contained in a column of air precipitates out. Hence, under warmer atmospheric conditions, increases in extreme precipitation events could be expected. This mechanism, governed by the Clausius-Claperyon relationship, is much simpler than the complex energy balance relationship expected to be responsible for changes in the mean hydrologic cycle (Allen and Ingram, 2002). As a result, changes in mean precipitation are poorly correlated with changes in precipitation extremes. In figure 2a, the change in the multi-model twenty year return value of annual maximum daily averaged precipitation from the end of the twentieth century (1990-1999) to the end of the twenty-first century (2090-2099) is shown under the A1B SRES scenario forcing conditions. In this map, the changes are shown as a fraction of the 1990-1999 values to better portray both moist and dry regions in the same figure. As with surface air temperature extremes, increases are widespread although there are a few noticeable areas of decreases over some deserts and eastern oceans. Over much of the land mass, 15% to 25% increases in the twenty year return value are predicted. The associated increase in frequency of large events is less for precipitation than it is for surface air temperature. In figure 2b, the number of times on average over a twenty year period that the 1990-1999 daily precipitation

return value levels would be reached under the SRES A1B 2090-2099 forcing conditions is shown. Over northern hemisphere land masses, these present day rare precipitation events would be reached about three times more often under 2090-2099 SRES A1B conditions as opposed to ten times more often for similar rare events of high surface air temperature.

The general features of the mean model extreme value changes are reproduced in the four individual models that have available ensembles of more than two realizations. Although not shown here, each of the models predicts large changes in surface air temperature return values over continental land masses. Following the behavior of predicted changes in decadal mean surface air temperatures, MIROC3.2 predicts surface air temperature return value changes considerably larger than the mean model while CCSM3.0, MRI3.2 and PCM exhibit less sensitivity to forcing changes than does the mean model. Similarly consistent with decadal mean temperature changes, precipitation return value changes are predicted to increase over widespread areas of the globe by the individual models. Those models exhibiting larger temperature sensitivity to forcing changes, such as MIROC3.2, show significantly larger increases in precipitation return values than those with lower sensitivities, such as PCM. This is consistent with the Clausius-Claperyon mechanism suggested by Allen and Ingram (2002). Also similar to the mean model, the individual model ensembles exhibit low correlation between precipitation mean value and extreme value changes.

The projected likelihood of changes in extreme weather events as the mean climate changes over the course of the coming decades is high.

In assessing the statistical significance of these extreme value changes, one must consider two related but distinct aspects of the available sample size. The first concerns the accuracy of the estimation of the three GEV parameters. Using a Monte Carlo approach (Hoskins and Wallis, 1997), reveals that changes of the magnitudes encountered under a century of SRES A1B forcing are highly significant to uncertainty in the estimation of the GEV parameters (Wehner, 2004). A second source of uncertainty, not addressed by this technique, comes from the internal variability of the climate system and the model's ability to simulate it. For if one were to repeat all the integrations with slightly perturbed initial conditions, a completely different parent distribution of daily values would be obtained. Until a much larger database of simulations is available, this question of the stability of the sample must be delayed.

Atmospheric component model resolution is relatively coarse in all of the IPCC AR4 models. This is more of an issue in the analysis of precipitation extremes than it is for surface air temperature extremes. By definition, extreme precipitation events are the result of individual storms. At horizontal resolutions exceeding a hundred kilometers, storm fronts are weakly represented by the models if at all. Preliminary analysis suggests a strong dependence of precipitation return value on horizontal resolution. Much larger values are obtained in models with greater spatial resolution and are in better agreement with observations.

Datasets to validate model simulation of extremes are quite limited and the variations between models are large (Kharin, et al 2005). Nonetheless, in the IPCC AR4 models considered here, a consistent pattern of statistically significant and large changes in precipitation and surface air temperature extremes is found.

Acknowledgements:

This work was performed under the auspices of the U.S. Department of Energy by the Lawrence Berkeley National Laboratory under contract No. DE-AC03-76SF00098 (LBNL). Partial support was provided by the National Science Foundation and the U.S. Department of Energy as a Climate Model Evaluation Project (CMEP) grant, # NSF ATM 0448921 and is supported as a U.S. Climate Variability and Predictability Program (CLIVAR) activity. We acknowledge the international modeling groups for providing their data for analysis, the Program for Climate Model Diagnosis and Intercomparison (PCMDI) for collecting and archiving the model data, the JSC/CLIVAR Working Group on Coupled Modeling (WGCM) and their Coupled Model Intercomparison Project (CMIP) and Climate Simulation Panel for organizing the model data analysis activity, and the IPCC WG1 TSU for technical support. The IPCC Data Archive at Lawrence Livermore National Laboratory is supported by the Office of Science, U.S. Department of Energy.

References

Allen, M. R., and W. J. Ingram, 2002: Constraints on future changes in climate and the hydrologic cycle. *Nature*, " , 224-232.

Castillo, E., 1988: Extreme Value Theory in Engineering. Academic Press, 408 pp

Easterling D.R., J.L. Evans, P.Ya. Groisman, T.r. Karl, K.E. Kunkel and P. Ambenje, 2000: Observed variability and trends in extrme climate events. *Bull. Am. Met. Soc.*, ***81***, *417-425*.

Hosking, J. R. M., and J. R.Wallis, 1997: Regional Frequency Analysis, An Approach Based on L-Moments, Cambridge University Press, 224 pp.

Kharin, V.V., F.W. Zwiers, and X. Zhang, 2005: Intercomparison of near surface temperature and precipitation extremes in AMIP-2 simulations, reanalyses and observations. *Journal of Climate*, in press.

Leadbetter, M.R., G. Lindgren, H. Rootzen, 1983: Extremes and related properties of random sequences and processes. Springer Verlag 336pp

Taylor, K.E., P.J. Gleckler, and C. Doutriaux, 2005: Tracking changes in the performance of AMIP models, in The Second Phase of the Atmospheric Model Intercomparison Project (AMIP2): Toward Innovative Model Diagnostics, Edited by P.J. Gleckler, WCRP report, in preparation.

Wehner, M.F. ,Predicted 21st century changes in seasonal extreme precipitation events in the Parallel Climate Model, *J. Climate* (2004) 4281-4290

Zwiers, F. W., and V. V. Kharin, 1998: Changes in the extremes of the climate simulated by CCC GCM2 under CO2 doubling. *J. Climate*, , 2200-2222

The Probabilistic Projection of Climate Risk

David B. Enfield[1] and Luis Cid-Serrano[2]
[1]NOAA Atlantic Oceanographic and Meteorological Laboratory, Miami, FL, 33149 USA. [david.enfield@noaa.gov]
[2] Statistics Department, Universidad de Concepción, Concepción Chile [lucid@udec.cl]

The last 15 years have seen much research on decadal to multi-decadal (D2M) climate modes and their global and regional impacts. At least some of these D2M modes suggest compelling climatic and ecological impacts. Both the Pacific Decadal Oscillation (PDO) and the Atlantic Multidecadal Oscillation (AMO) are associated with alternating trans-decadal regimes in precipitation and drought frequency, which appear to be sensitive to small but persistent changes in the prevalent atmospheric circulation patterns over the continental regions adjacent to the oceans that mediate the oscillations. They have also been shown to modulate (render nonstationary) the rainfall signatures of El Niño-Southern Oscillation (ENSO) in the United States and they are reflected in the multidecadal changes in North Pacific fisheries. Of concern for climate applications is the fact that — unlike El Niño-Southern Oscillation (ENSO) — numerical models have proven incapable of predicting future phase shifts of D2M climate modes in a deterministic manner.

The alternatives to such predictions are probability-based projections, but these are hampered because the instrumentally based time series are limited to the last 130-150 years, which yield too few realizations of D2M cycles for conventional statistical approaches to deal with. There are two ways to approach the lack of suitable observational data sets: (1) applying Monte Carlo-style resampling techniques to the climate index data and (2) analyzing longer, multi-century proxy reconstructions, based mostly on tree rings. To illustrate this, we apply both approaches to the problem of projecting the risk of a future shift in the AMO. By

Continued on Page 12

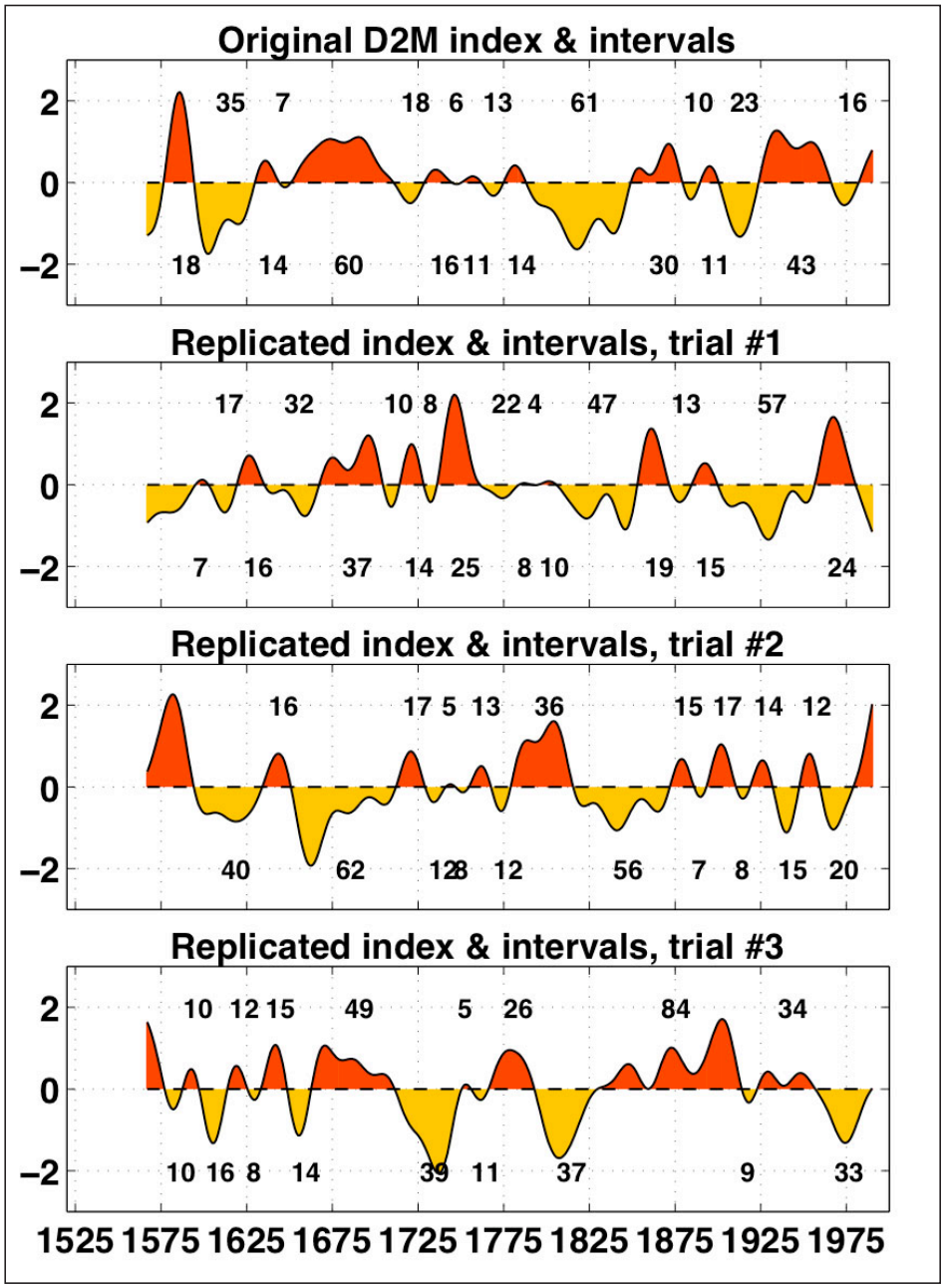

Fig. 1. Upper panel: Smoothed annual tree ring reconstruction of the Atlantic multidecadal oscillation (AMO) index by Gray et al. (2004). Lower panels: Smoothed resampled versions of the Gray et al. index using randomization in the frequency domain (Ebisuzaki 1997). Numeric annotations are the intervals (years) between zero crossings.

Calendar of CLIVAR and CLIVAR-related meetings

Further details are available on the U.S. CLIVAR and International CLIVAR web sites: www.usclivar.org and www.clivar.org

Development of Improved Observational Data Sets for Reanalysis

!) 0: =07 - 0; #
Greenbelt, MD
Attendance: Open
Contact: Kathy Regul (kregul@infonet-ic.com)

CLIVAR/OOPC/GOOS/ARGO Workshop on the South Pacific

" ' . =9- 0; #
Concepcion, Chile
Attendance: Limited
Contact: CLIVAR Office (icpo@soc.soton.ac.uk)

Tropical Atlantic Variability Workshop

' . =9- 0; #
Venice, Italy
Attendance: Invited
Contact: Paola Malanotte-Rizzoli (Rizzoli@mit.edu)

CRCES Workshop on Decadal Variability

' . =9- 0; #
West Virginia, USA
Attendance: Open
Contact: http://www.crces.org

NOAA Climate Diagnostics and Prediction Workshop / Climate Test Bed Meeting

" ' . =9- 0; #
State College, Pennsylvania
Attendance: Open
Contact: www.cdc.ncep.noaa.gov

Greenhouse 2005: Action on Climate Change

! &9?07 - 0; #
Melbourne, Australia
Attendance: Open
Contact: www.greenhouse2005.org

International Repeat Hydrography Workshop

" &9?07 - 0; #
Shonan Village, Japan
Attendance: Invited
Contact: http://ioc.unesco.org/ioccp/about.htm

AMMA 1st International Conference

&9?07 - 0; " 0. 07 - 0; #
Dakar, Africa
Attendance: Open
Contact: www.amma-international.org/conferences/dakar2005

AGU Fall Meeting

 # 0. 07 - 0; #
San Francisco, CA
Attendance: Open
Contact: http://www.agu.org/meetings/

American Meteorological Society Annual Meeting

, 8>, ;B 0- ;>, ;B
Atlanta, Georgia
Attendance: Open
Contact: www.ametsoc.org

U.S. CLIVAR Town Hall Meeting

! , 8>, ;B
Atlanta, Georgia
Attendance: Open
Contact: www.usclivar.org

U.S. CLIVAR Committee Meeting

0- ;>, ;B
Atlanta, Georgia
Attendance: Invited
Contact: www.usclivar.org

13th Ocean Sciences Meeting, a joint meeting of ASLO, TOS and AGU

" 0- ;>, ;B
Honolulu, HI
Attendance: Open
Contact: http://www.agu.org/meetings/

U.S. CLIVAR Salinity Working Group Meeting

" # 0- ;>, ;B
Honolulu, HI
Attendance: Invited
Contact: www.usclivar.org

ARGO 2nd Science Workshop

! , ;. 3
Venice, Italy
Attendance: Open
Contact: http://www.argo.ucsd.edu/frsecond_science_work.html

Workshop Tropical Cyclones and Climate

, ;. 3
IRI, Palisades, NY
Attendance: Open
Contact: http://iri.columbia.edu/outreach/meeting/tropicalcyclones

Continued from Page 10

then adjusting a probability model to the distribution of resampled AMO phase intervals, we extract a practical method for determining the risk of a future departure from the current AMO climate regime. In lieu of non-existent deterministic predictions, this method provides a statistically-based guide for the development of decision support tools for managers and stakeholders in sectors affected by D2M climate modes, such as agriculture, water, energy, health and disaster risk.

To illustrate the methods, we use the unsmoothed 424-year annualized index of the AMO reconstructed from tree rings in North America and Europe (Gray et al. 2004), calibrated against the AMO index suggested by Enfield et al. (2001). To eliminate unwanted short-interval variability, the time series are then smoothed with a Butterworth filter of order 8 and a half-amplitude response cutoff at 15 years. To increase the sample size we randomly resample the index multiple times, each time transforming the original time series into the frequency domain, randomizing the Fourier phases, and reverse transforming back to the time domain. Unlike most randomizations in the time domain, this method preserves the original power spectrum, but still produces resampled series whose temporal correlations with each other and the original series are expected to be zero on average. Fig. 1 (top panel) shows the smoothed AMO reconstruction, annotated with the climate regime intervals between zero crossings, plus similar plots for three randomly resampled versions of the data. The assumption implicit in this resampling is that the original series is extracted from a larger population (longer duration) with time-invariant statistics (stationary).

The histogram of Fig. 2 (top) illustrates a typical empirical distribution of AMO climate regime intervals produced by extracting five new time series from the original Gray et al. (2004) spectrum. The distribution is fit by the smooth curve, which corresponds to a gamma pdf whose shape (A) and scale (B) parameters are adjusted to the data by maximum likelihood estimation (MLE). As in the example shown, a Kolmogorov-Smirnov (KS) goodness-of-fit test is applied to the cumulative distribution (cdf, lower panel) and usually shows the fit to be acceptable at the 95% level of significance. Each new fivefold resampling results in varied but similar parameter estimates. To obtain a stable estimate of the gamma distribution for the 424-year period, we average the parameter estimates from 50 resamplings, obtaining A = 1.93 and B = 10.3. These values are later used to project the risk of future climate regime shifts.

If we divide the longer index series into three segments of 141 years each and repeat the above procedure, we find that the distribution parameters differ significantly from one segment to another, which means that the AMO process is not stationary. This does not invalidate the estimation procedure, but it means that the distribution parameters are more uncertain than implied by the 50-member spread for the longer 424-year estimation. By pooling the 150 parameter pairs for the three segments, we can estimate the uncertainty of the underlying distribution more realistically. We will return to this in a later section.

, 54 82 =30 : ;9 0. =98 <

If we let P(□) represent the probability of a realization □ within the population space of the stochastic climate regime intervals (T), we can then construct useful probability projections for future realizations, based on the estimated gamma parameters for the intervals between zero crossings of the AMO index. For example, the conditional probability that a future climate regime shift will occur within t_2 years, given that t_1 years have elapsed since the last, opposite regime shift, may be expressed as

$$P(T > t_1 \cap T \quad t_1 + t_2 \mid T > t_1) = P(T > t_1 \cap T \quad t_1 + t_2)/P(T > t_1)$$
$$= P(t_1 < T \le t_1 + t_2)/P(T > t_1)$$
$$= (\Gamma[t_1 + t_2] - \Gamma[t_1])/(1 - \Gamma[t_1]) \qquad \text{Eq. 1}$$

where $t = t_1 + t_2$ is the current climate regime interval and □[t] is the estimated gamma cdf. A reasonable, further refinement of this statement is to ignore the probability space for very short intervals (five years or less) that would normally be ignored in practice in retrospective analysis. This is accomplished by using a truncated gamma in Eq. 1, □[t] = □ [t]/(1-□ [5]), where $t > 5$.

Fig. 3 shows the probability P(□) as a function of t_1 (abscissa) and t_2 (ordinate). An example of using this calculation is as folllows. It is generally thought that the AMO switched from cool to warm during the 1994-95 time frame. If we use Fig. 3 with t_1 = 10 years, i.e. the number of years that have elapsed since that time, we find a rather low probability (< 30%) that the AMO will switch back to its cool phase in less than t_2 = 5 years from now. For t_2 = 10 and 15 years, the risk increases to ~51% and ~70%, respectively, while a climate regime shift within 20 years is highly likely (~86%). Based on current research, such a shift would be associated with a return to more frequent droughts in Florida, fewer droughts in the Colorado River basin, and less frequent severe hurricanes in the tropical Atlantic. As expected, Fig. 3 shows that the risk for any of these t_2 values increases as time advances and the last climate regime shift recedes further into the past (t_1 increases).

The uncertainty of such estimates can be derived from the parameter estimates of the three Gray et al. (2004) time segments, which collectively have a considerably larger spread than those of the 424-year estimation used for Fig. 3. This is primarily due to the nonstationarity of the intervals over the last half millennium. Pooling the 3x50 segment estimates of A and B, we randomly select a large number of parameter values within their overall 1-□ confidence intervals and generate the corresponding rms uncertainty in P(□) over the domain of Fig. 3. The uncertainty is fairly uniform over the [t_1,t_2] domain shown. For confidence intervals between 95% and 99%, the uncertainty ranges between ±2% (□=0.05) and ±5% (□=0.01), respectively.

We have not fully explored the uncertainties that attend such projections. Besides the uncertainty associated with

natural nonstationarity, it is also desirable to consider how the quality of the reconstruction will affect the distribution parameters. Where multiple reconstructions of the same climate index are available (at least four exist for the PDO) the uncertainty due to the inability of the reconstructions to perfectly emulate the climate process can be estimated by applying the above methods to the multiple reconstructions, rather than to segments of a single reconstruction. Only one reconstruction yet exists for the AMO, so we have not done this.

Fig. 3 is only one example of a potentially useful climate risk projection tool. Thus for any given year in which decisions are made, one can also construct a graph showing the distribution for $P(t_a < T \le t_b)$, where t_a (abscissa) and t_b (ordinate) define a time range, e.g. 10-15 years into the future. The present risk of an AMO shift between t_a = 2015 AD and t_b =2020AD is about 19%. Such a graph can be transformed from Fig. 3 by subtacting the probability for t_1=10, t_2=t_a from that of t_1=10, t_2=t_b.

The application illustrated here has its limitations. One is that it uses the zero value of the index to separate just two states—above and below zero. This allows the possibility of classifying as a climate regime an interval where the index may not rise significantly above a value critical for impacts to occur. It is obviously advisable that the method be modified to account for neutral range as well as high and low ranges beyond appropriate thresholds.

Other, more esoteric projections can be developed. McCabe et al. (2004) have shown how the uncorrelated +/- phases of the PDO and AMO have juxtaposed since the mid-19th century in ways that plausibly explain mega droughts in the southwestern and Midwestern U.S. If both oscillations can be statistically modeled as we have done here only for the AMO, it is possible to develop joint probability projections for the four possible phase-phase scenarios (+/+. +/-. -/-. -/+), under the assumption that the climate oscillations are mutually independent. It is also possible to query the conditional probability for regime interval magnitude or intensity — based on the index area subtended between zero crossings

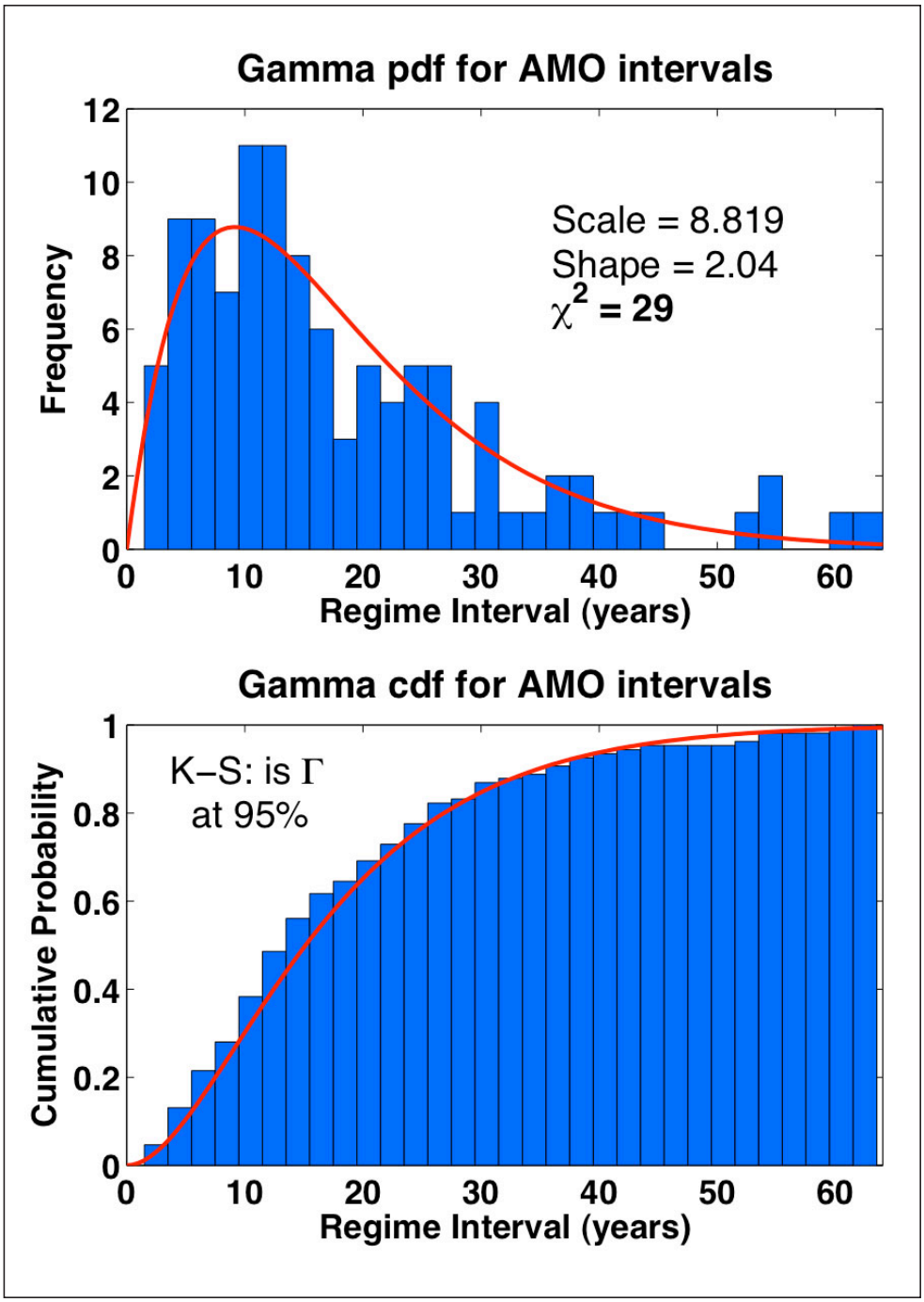

Fig. 2. Upper panel: histogram (vertical bars) of zero crossing intervals from a set of five resampled and smoothed versions of the Gray et al. (2004) index and the maximum likelihood (MLE) gamma probability distribution (solid curve) fit to the histogram. Lower panel: cumulative empirical distribution (vertical bars) and gamma cumulative distribution function (solid curve), indicating that the Kolmogorov-Smirnov goodness-of-fit criterion is satisfied at the 95% significance level.

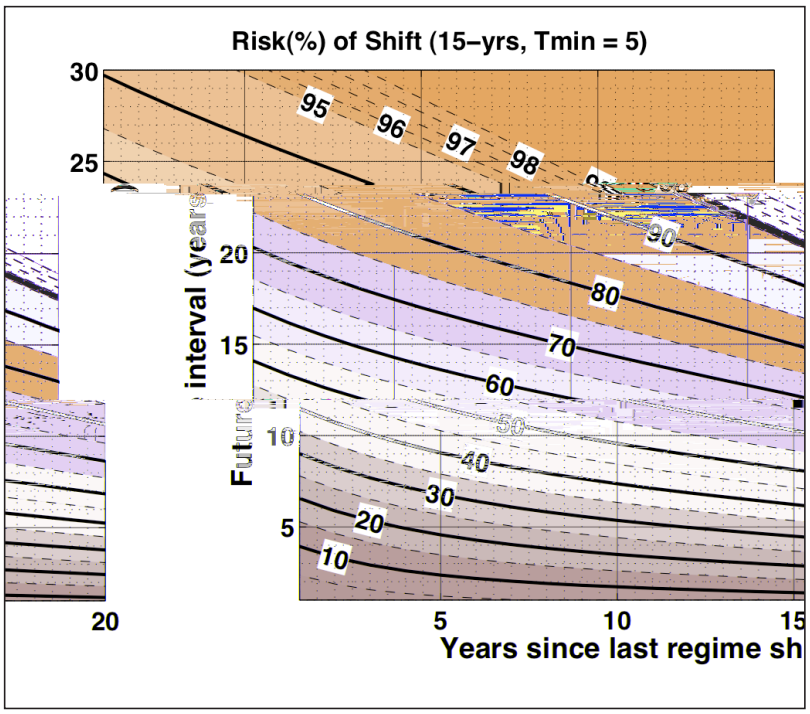

Fig. 3. Distribution of the probability of an AMO regime shift occurring wthin t_2 future years (ordinate) given that t_1 years (abscissa) have elapsed since the last regime shift. Based on the gamma distribution with scale and shape parameters of 10.3 years and 1.93, truncated for $t_1 + t_2 >$ 5 years (see text).

— given an interval of a certain length.

) >7 7 , ; B, 8/ / 4< ><<498

We have shown how a multi-century proxy reconstruction of a climate index may be used to estimate the pdf of climate regime intervals, thus providing a basis for the projection of climate risk and the eventual development of useful decision support tools. The spectrum preserving resampling of the time series provides sufficient sample sizes for pdf estimation using the gamma distribution. We have given a detailed example of a derived climate risk projection and have suggested others that can be developed.

Consider the situation in 1990, more than 20 years into a period of cool North Atlantic sea surface temperatures (AMO) associated with dry conditions in Florida, wet conditions in the southwestern region and less frequent hurricanes. It is not difficult to imagine management decisions that could have been made then as an AMO reversal became imminent within operational time horizons. Where water was expected to become more plentiful, flood control measures could have been implemented and development on flood plains discouraged. Where more persistent and/or frequent droughts were expected, more water could have been shunted to aquifer storage, water access leases shortened, reservoir withdrawals reduced, conservation measures implemented and agricultural practices modified. Underwriting associations could have increased the funding of windstorm contingency pools in anticipation of more frequent, destructive hurricanes.

D2M climate risk assessment is not useful only when a climate shift becomes imminent. In general, for any policy or measure that can be adopted in anticipation of a change, there exists an alternative to be followed if the probability of change is low. Policies may be reviewed periodically in light of changing probabilities and the spectrum and effectiveness of available mitigation measures can be revised on a regular basis. Cognizance of the changing nature of climate and its impacts is a relatively recent development and it has taught us that effective management should not be based on static policies. Perhaps the best example of this lesson is the recent increase in destructive hurricane potential related to the change in the AMO climate regime and its impact on the insurance industry.

It is important to point out that the usefulness of these methods for actual applications will depend on the nature of the application, the strength of the connection between the climate mode and the target variable, and managers' ability to utilize the projections in making operational decisions. In general, the closer the relationships of the modeled index to the decision-triggering target variables, the better. Thus, if a proxy reconstruction of stream flow exists, this may be more useful to model than the climate mode whose association with the stream flow is less than perfect. However, projections based on a climate mode have the advantage of being appropriate over a wider range of applications and geographic regions.

Finally, the ultimate uncertainty for which there is no sure remedy at present, is the effect that global climate change will have on future climate regime characteristics. However, it is worth noting that if the true future distribution parameters are different from those in the past, the effect on risk projection (as shown in Fig. 3) is to shift all probabilities in the same direction and by similar amounts. Hence, the relative change in probability from one part of the domain to another is little affected by a parameter discrepancy. Arguably, the evolving *change* in risk is more likely to influence management and policy adjustments, than is the absolute risk at a given position, as long as the errors are within reasonable bounds. In fact this principle applies to all sources of uncertainty.

References

Enfield, D. B., A. M. Mestas-Nuñez, and P. J. Trimble, 2001: The Atlantic multidecadal oscillation and its relation to rainfall and river flows in the continental *U.S. Geophys. Res. Lett.*, , 2077-2080.

Gray, S. T., J. L. Graumlich, J. L. Betancourt, and G. T. Pederson, 2004: A tree-ring based reconstruction of the Atlantic Multidecadal Oscillation since 1567 A.D. *Geophys. Res. Lett.*, ! , L12205, doi:10.1029/ 2004GL019932.

McCabe, G. J., M. A. Palecki, and J. L. Betancourt, 2004: Pacific and Atlantic Ocean influences on multidecadal drought frequency in the United States. *Proc. Nat. Acad. Sci.*, , 4136-4141.

Report on First U.S. CLIVAR Summit

by David M. Legler Director, U.S. CLIVAR

Over 50 U.S. CLIVAR Panel members (including representatives from the previous regional panels), interested scientists, and agency representatives attended the first U.S. CLIVAR Summit, August 15-20, in Keystone, Colorado (ironically, in Summit County!). Everyone enjoyed the scenic location and availability of nearby recreational diversions during this inaugural meeting of the reorganized U.S. CLIVAR. Unfortunately, rockslides on the interstate between Denver and Keystone made for longer driving trips for many.

The purpose of the Summit was to consider and chart the future of the U.S. CLIVAR program in the three broad areas that correspond to our new Panels: Phenomena, Observations, and Syntheses (POS), Process Studies and Model Improvement (PSMI), and Predictability, Predictions, and Applications Interface (PPAI) and to continue forward momentum of activities in various stages of planning and implementation. The first portion of the meeting focused on highlighting the national, international, and agency program context of CLIVAR, and important linkages to U.S. CLIVAR. GEWEX and the Ocean Carbon Cycle provided updates on their programs and suggested areas for potential linkages to U.S. CLIVAR. The Panels (Table 1) were then charged to develop long-term and near-term objectives, determine the scientific activities required to achieve these objectives, and identify specific Panel actions that will be undertaken to facilitate progress. Additionally, the Panels were asked to consider how activities in various stages of planning and implementation will (or could) contribute towards these objectives and how these activities should move forward. The Panels met individually, with each other, and with agency program managers over the course of a few days to begin building their strategic visions, identifying issues common to more than one Panel, and discussing a range of specific activities. They also discussed topics for Working Groups (small, focused groups, with limited lifetime) to accelerate implementation and coordination in critical areas.

Phenomena, Observations, and Syntheses (POS)	John Marshal (MIT), Sumant Nigam (Univ of Maryland)
Process Studies and Model Improvement (PSMI)	Meghan Cronin (PMEL), Paul Schopf – interim (George Mason University)
Predictability, Predictions, and Applications Interface (PPAI)	Lisa Goddard (IRI), Alex Hall (UCLA)

Table 1: List of U.S. CLIVAR Panels and Co-Chairs

The Panels presented their plans and recommendations (which were still very much in draft form) in plenary. The initial issues and objectives the Panels considered and raised at the Summit were very exciting and resonated with the agencies. The Panels embraced the historical directions of the program and also took great steps towards identifying overarching objectives that covered a range of time scales from subseasonal to decadal and longer, vexing challenges for which community-wide engagement is required, and phenomena of great interest to the scientific and decision-making communities for which we need additional research to understand, characterize, assess predictability of, and develop prediction capabilities. Agency program managers provided very positive feedback on the planning achieved at the Summit and encouraged the Panels to move forward quickly to flesh out their plans.

The three Panels are now carefully building on their Summit discussions, and talking to other Panels so that a cogent and balanced strategy is developed. The Panels will be completing brief written strategy documents over the next several months. Our plan is to complete draft overviews of Panel plans this Fall after which they will solicit community (both national and international) input and reactions as we begin to more fully engage the agency programs and the community to address the challenges identified in these plans.

Progress towards these community plans can be monitored through the U.S. CLIVAR web site (www.usclivar.org). Announcements about the availability of draft US CLIVAR strategies will be distributed through emails. We encourage the community to provide feedback to these planning efforts through the U.S. CLIVAR Office, through our web page, or through the Panel co-chairs and Panel members.

U.S. CLIVAR Salinity Working Group

The first working group formed under the restructured U.S. CLIVAR is the Salinity Working Group, which will hold its first meeting following the Ocean Sciences Meeting 2006 on February 24-25 in Honolulu, Hawaii. The Salinity Working Group is tasked with reporting to the Phenomena, Observations and Synthesis Panel of U.S. CLIVAR within the first year of the group's commencement. The working group has several objectives including:

- describing the role of ocean salinity in the global water cycle, global ocean circulation and climate variability;
- providing guidance to NASA and the international community on observational and scientific activities to be considered in advance of and during the Aquarius mission;
- identifying the requirements and challenges for analyzing, observing, and monitoring salinity.

In order to meet these objectives, the working group will host a special session at AGU's Ocean Sciences 2006 Meeting in Honolulu, Hawaii. The special session, entitled *The Role of Ocean Salinity in Climate*, will be moderated by the working group co-chairs James Carton (University of Maryland) and Ray Schmitt (Woods Hole Oceanographic Institute) and working group member Gary Lagerloef (Earth and Space Research). Papers for this session are encouraged to look at understanding the importance of salinity in climate variability, especially (1) the influence of salinity variability on tropical dynamics and ENSO; (2) large scale salinity changes in mid to high latitudes that influence ocean convective overturning circulation; and (3) closure of the global ocean-atmosphere freshwater balance. The abstract deadline for Ocean Sciences 2006 is 20 October 2005. Meeting and abstract information is located at www.agu.org/meetings/os06.

Additional information regarding the U.S. CLIVAR Salinity Working Group (including membership) can be found at: www.usclivar.org/Organization/SalinityWG.html.

U.S. CLIVAR OFFICE
1717 Pennsylvania Avenue, NW
Suite 250
Washington, DC 20006

Subscription requests, and changes of address should be sent to the attention of the U.S. CLIVAR Office (usco@usclivar.org)